Journal Pre-proof

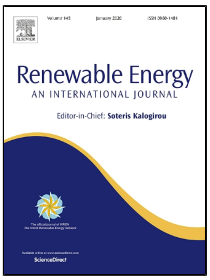

Impact of global warming on photovoltaic power generation over West Africa

Windmanagda Sawadogo, Babatunde J. Abiodun, Emmanuel C. Okogbue

PII:	S0960-1481(19)31713-6
DOI:	https://doi.org/10.1016/j.renene.2019.11.032
Reference:	RENE 12579
To appear in:	*Renewable Energy*
Received Date:	13 June 2019
Accepted Date:	08 November 2019

Please cite this article as: Windmanagda Sawadogo, Babatunde J. Abiodun, Emmanuel C. Okogbue, Impact of global warming on photovoltaic power generation over West Africa, *Renewable Energy* (2019), https://doi.org/10.1016/j.renene.2019.11.032

Impact of global warming on photovoltaic power generation over West Africa

Windmanagda Sawadogo[1 2], Babatunde J. Abiodun[2] and Emmanuel C. Okogbue[3]

[1] West African Science Service Center on Climate Change and Adapted Landuse (WASCAL), Graduate Research Program on West African Climate System, Federal University of Technology, Akure, Nigeria

[2] Climate System Analysis Group, Department of Environmental and Geographical Science, University of Cape Town, Cape Town, South Africa

[3] Department of Meteorology and Climate Science, Federal University of Technology, Akure, Nigeria

Corresponding author: sawadogowind@gmail.com

Abstract

Many West African countries are plagued with poor electricity. The abundance of solar irradiance over the region makes solar energy an attractive solution to the problem, but there is a dearth of information on how the ongoing solar dimming and global warming may alter the solar energy over the region in the future at various global warming levels. This study investigates the impact of climate change on photovoltaic power generation potential (PVP) over West Africa under four global warming levels (1.5°C; 2.0°C; 2.5°C and 3.0°C) and under the representative concentration pathway 8.5 (RCP 8.5) climate change scenario. Fourteen regional climate model simulations from the Coordinated Regional Climate Downscaling Experiment (CORDEX) were analysed for the study. The capability of the simulations to reproduce the PVP and climate variables over West Africa is quantified. The results show that the CORDEX simulation ensemble captures the spatial distribution and the annual cycle of climate variables and PVP over West Africa, though with few biases. The simulation and observation indicate that PVP over West Africa ranges from 8% to 25% and the annual cycle is influenced by the seasonal variation of the monsoon system. The simulation ensemble projects a decrease of PVP over West Africa in the future and indicates that the magnitude of the decrease grows with warming levels. The maximum decrease in PVP projected over any country or zone in the region is less than 3.8% even for a warming level of 3.0°C. Hence, the study suggests that ongoing global warming may have an influence on PVP over West Africa.

Keywords: Solar energy; Global warming; Global dimming, West Africa; Paris agreement

1. Introduction

Access to electricity is a big challenge in many West African countries. For example, more than 40% of the population in Nigeria (the most populous country in Africa) have no access to electricity (IEA, 2017). In Senegal, more than 50% are without electricity. The percentage (about 80%) is even higher in countries like Liberia, Sierra Leone, Niger, and Burkina Faso (IEA, 2014). The main reason for this problem is lack of infrastructures caused by financial issues and poor electricity production from hydropower and thermal power plants, which are the major sources of electricity generation. Some hydropower plants do shut down due to the lack of water. For instance, in 1998, unavailability of water in the Akosombo Dam led to electricity outages in Ghana, Togo, and Benin. As much happened in Nigeria in 2001 when the largest dam in the country (Kainji Dam) experienced drought. This also recurred in Senegal, Mali, and Guinea for years

(Gnansounou, 2008). The West African countries that generate their electricity from thermal power also experience power cuts due to the difficulty of fuel procurement (Gnansounou, 2008). Hence, the need to reduce the crippling impacts of lack of electricity on the socio-economic developments in West Africa has called for more studies on other sources of electricity, especially on more reliable and more environmentally friendly energy sources.

Solar energy is a good alternative source of electricity generation in West Africa, one of the sunniest regions in the world. In West Africa, the daily average solar radiation is estimated to be about 5-6 kWh m^{-2} throughout the year. Hence, to harness the potential solar energy for electricity, various countries are now building solar photovoltaic (PV) power plants, the most well-deployed and well-used solar energy technology for powering households, buildings, streetlights and community centres. For instance, at the end of 2017, Burkina Faso inaugurated one of the largest solar PV power plants in West Africa with 33 MW, and Senegal has an installed capacity of 50 MW electricity from PV solar power. In addition, as part of climate change mitigation strategy, the Economic Community of West African States (ECOWAS) Members States, has decided to invest about 1,773 Million Euros in solar PV for electricity generation by 2030 (ECREEE, 2015). However, the success of this ambitious solar energy project depends on future climate, because the solar PV generation depends on climate variables like temperature and solar irradiance (Zhou et al., 2007). Given that PV power declines with an increase in solar cell temperature and cloudiness and also with a decrease in irradiance levels (Ishii et al., 2013), there is a concern that the ongoing global warming may have negative impacts of solar PV energy. Hence, there is a need for reliable information on the potential impacts of climate change on solar PV technology over West Africa. Such information will guide the policymakers on solar energy investment.

The need to mitigate the impacts of climate change in various socio-economic activities has led the United Nations Framework Convention on Climate Change (UNFCCC) to reach an agreement called the Paris Agreement. The Paris Agreement aims to reduce the global carbon footprint and keep the global mean temperature (GMT) rise below 2°C (and even further to 1.5°C) above the pre-industrial (PI) level (UNFCCC, 2015). To support the agreement, Hulme (2016) has advocated for more studies on the relative impacts global warming at 1.5 and 2°C global warming levels (GWLs) and few studies have evaluated the impacts over West Africa. For instance, Diedhiou et al (2018) found that the projected increase in frequency and duration of heat waves over West Africa at 2.0°C GWL is much higher than that of 1.5°C. Kumi and Abiodun (2018) projected a

delay in the rainfall onset day and shorter length rainy season over most parts of West Africa at both warming levels, but the magnitude of the projection is higher at 2°C than at 1.5°C GWL by more than 10 days. In contrast, Klutse et al (2018) found no significant difference in the magnitude projected decrease consecutive wet days at 2°C than 1.5°C GWLs. In energy sector, Sawadogo et al (2019) projected an increase in wind power density (WPD) over West Africa and the increase in WPD increases with the warming levels. However, there is a lack of information on how global warming levels may impact the PV power generation potential (hereafter PVP) over the West Africa region.

Several studies have investigated the potential impacts of climate change on solar radiation (and on the PV power output) and found different results over various regions of the world (e.g., Burnett et al., 2014; Crook et al., 2011). While some studies projected that climate change may increase solar irradiance, others indicated that it may reduce the resource. For instance, Burnett et al. (2014) projected that climate change may increase solar irradiance (by 3.4% in the 2050s and 4.4% in the 2080s) over the UK. Panagea (2014) also projected an increase (about 2-3 W/m^2 in 2011–2050 and 5 W/m^2 in 2051–2100) over Greece. In contrast, Jerez et al (2015) project a decrease (up to 14% by 2050) over most of the part of Northern European countries, and Crook et al (2011) projected a decrease over the Western USA (2 - 3.5%) and over Saudi Arabia (5%) by the end of the century. Over West Africa, using simulations from a general circulation model (ECHAM4), Huber et al (2016) projected a decrease in direct normal irradiance and global horizontal of about 20% and 5% respectively in a period of 2035-2039. Bazyomo et al (2016) projected a general decrease of PV power generation in West African countries over a period of 2006-2045. However, given that the focus of their projection was over a specific time period, the results may be difficult for policymakers to apply in the framework of the Paris Agreement, which requires the information at specific warming levels (1.5°C and 2.0°C). Furthermore, their projections are based on simulations from a single model, whereas robust information for policymakers requires multi-model ensemble mean projections. Also, there is a lack of information on how climate variables may contribute to the change in PVP over West Africa.

Hence, the present study aims to investigate the impact of climate change on PVP over West Africa at different global warming levels (1.5, 2.0, 2.5 and 3.0°C; under the representative concentration pathway 8.5 scenario, RCP8.5). The study analysed multi-model ensemble simulations from CORDEX and quantified the contribution of each variable in PVP equation to the projected changes in PVP over the subcontinent. The article is structured as follows. Section 2 describes the

data and methods used in the study, Section 3 presents and discusses the results, while Section 4 presents the conclusion of the study.

2. Data and method

2.1 Study Area

The study covers the entire West African domain but also focuses on the climate zones and countries in West Africa (Fig. 1). Following Abiodun et al. (2012), we divided the subcontinent into three zones accordingly: Guinean zone (18W:18E, 4N:8N), Savannah zone (18W:18E, 8N:12N), and Sahel zone (18W:18E, 12N:16N). At the country scale, we selected fourteen countries of the Member States of ECOWAS that have agendas to increase their electricity production with PV solar. For instance, Nigeria and Sierra-Leone target to increase their electricity capacity to 6,000 and 1,200 MW respectively by 2030 (ECREEE, 2016a; ECREEE, 2016b).

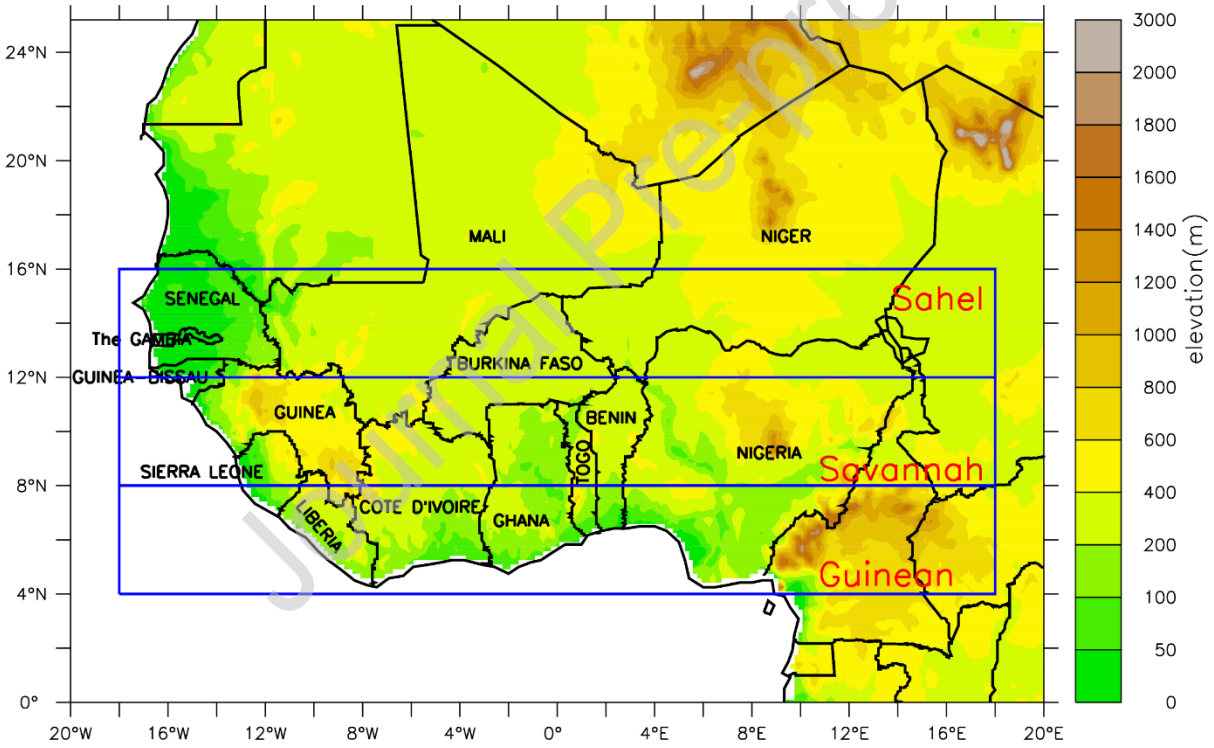

Figure 1: West African domain showing the topography (in metres) and the climatic zones delineated as Guinea, Savannah, and Sahel zones. The names of the West African countries used in the study are indicated.

2.2 Data

2.2.1 CORDEX dataset

The climate model simulations used for the present study come from the Coordinated Regional Climate Downscaling Experiment (CORDEX). CORDEX provides a framework to investigate

climate change impact scenarios at a regional scale (Nikulin et al., 2012). The spatial resolution of the CORDEX datasets is roughly 50km (0.44° x 0.44°). From the CORDEX datasets, we got daily surface-downwelling shortwave radiation (Rs; also called solar irradiance), air temperature (Ts), wind speed (Ws; at 10m above the ground level) and relative humidity (Rh). For the study, we used 14 simulation ensemble members obtained by downscaling by 9 Global Climate Models (GCMs) simulations with 3 Regional Climate Models (RCMs), as shown in Figure (2). To analyse the CORDEX simulations, we use the multi-model mean ensemble (henceforth Rmean). The Rmean is generally considered to have a better performance than an individual model (Samouly et al., 2018). The Rmean is formed by merging a number of models with equal weights and has been found to have a higher likelihood for a better score than any individual model (Wallach et al., 2016; Hagedorn et al., 2005). Moreover, the Rmean gives better results in terms of long-term climate change projection rather than an individual model (Houghton et al., 2001).

2.2.2 Generation of the global warming levels

For the climate change projection, we use the RCP8.5 because it does not integrate any specific climate mitigation target (business as usual; Van Vuuren et al., 2011). The greenhouse gas emissions and concentrations in this scenario increase considerably over time, leading to a radiative forcing of 8.5 W/m^2 at the end of the century (Riahi et al., 2011). For the climate change projection, we also use four global warming levels (1.5°C, 2.0°C, 2.5°C and 3.0°C; hereafter, GWLs: GWL1.5, GWL2.0, GWL2.5, and GWL3.0) above the PI level (1881-1910). The GWL1.5, GWL2.0, GWL2.5, and GWL3.0 is defined when the GMT reaches 1.5, 2.0, 2.5, 3.0°C respectively above the PI levels. To compute the 30-year GWL for each GCM simulation, we use 30-year centred at the year when GCM reaches the 1.5, 2.0, 2.5, 3.0°C in GMT relative to PI levels under the RCP 8.5 (Déqué et al., 2017). For the analysis, we used the same GWL period of the GCM to extract the 30-year of the GCM downscaled by the RCM using 1971-2000 as a control period. The names of the driving GCMs, the RCMs and the period of the GWLs used in this study are shown in Figure 2.

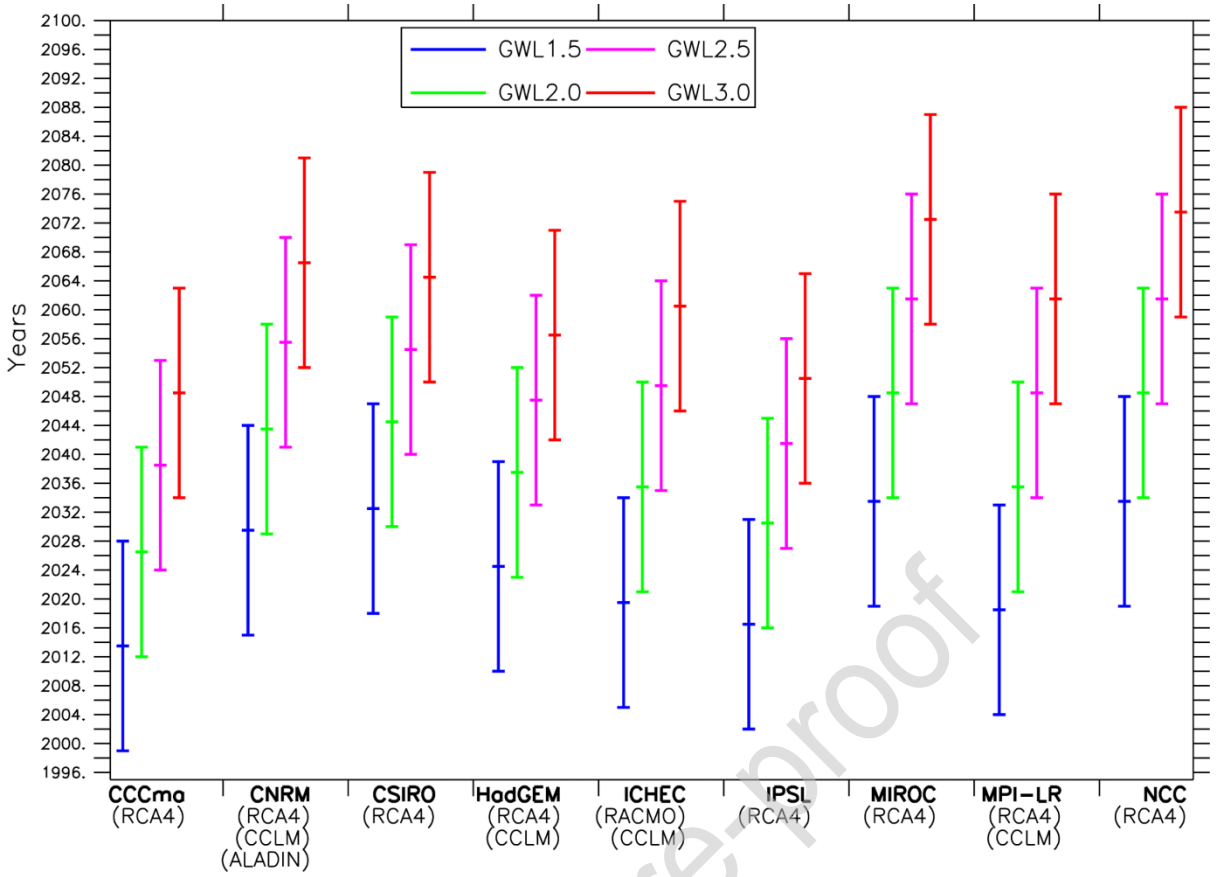

Figure 2: The extracted 30-year global warming period based on the method of Deque et al. (2016) under the RCP 8.5 scenario. The written bold indicates the driving GCM and the written bracket indicates the downscaling RCM used in this study. Each line denotes the start year (the bottom), the middle year (the median of the line) and the end year (the top) of the warming level.

2.2.3 Observation datasets description

For the model evaluations, we used three types of dataset. The first data is derived from the CM SAF second edition of the Surface Solar Radiation Data Set-Heliosat Edition 2 (SARAH-2) (Pfeifroth et al., 2018); hereafter SARAH. SARAH is a product derived from satellite-observations of the visible channels of the MVIRI and the SEVIRI instruments onboard the geostationary Meteosat satellites. It covers 33 years (1983-2015) and has a spatial resolution of 0.05° by 0.05°. Many studies have demonstrated the quality of the SARAH data through the Baseline Surface Radiation Network (Müller et al., 2015; Stöckli and Stöckli, 2013). Secondly, we used the temperature variable from the Climatic Research Unit (CRU) to evaluate the temperature of the Rmean. CRU is a monthly high-resolution gridded data (0.5° x 0.5°) using station data with a period ranging from 1901 to 2016. Finally, we use the ERA-Interim reanalyses dataset from the European Centre for medium-range weather forecasts (ECMWF; Dee et al., 2011). The ERA-Interim dataset has 0.75°x 0.75° horizontal grid size and extends from 1979 to the present date. From the ECMWF website, we retrieved surface wind speed (10m above the ground level) and

relative humidity which has been computed from dewpoint and specific humidity. The selected period for the three datasets (SARAH, CRU and ERA-Interim) ranges from 1985 to 2014. For the rest of the study, the three datasets are referred to as observations. The observations and simulations datasets were remapped to 0.44° x 0.44° grid points and presented on the annual and monthly average.

2.3 Method

The impact of climate change of PVP was considered by including the Rs, Ts, Ws and Rh over the West Africa region and its three climatic zones. Fig. 3 exhibits an overview of the study methodology. The evaluation and projection over a climatic zone are done by averaging the values over the grid points within the climatic zone.

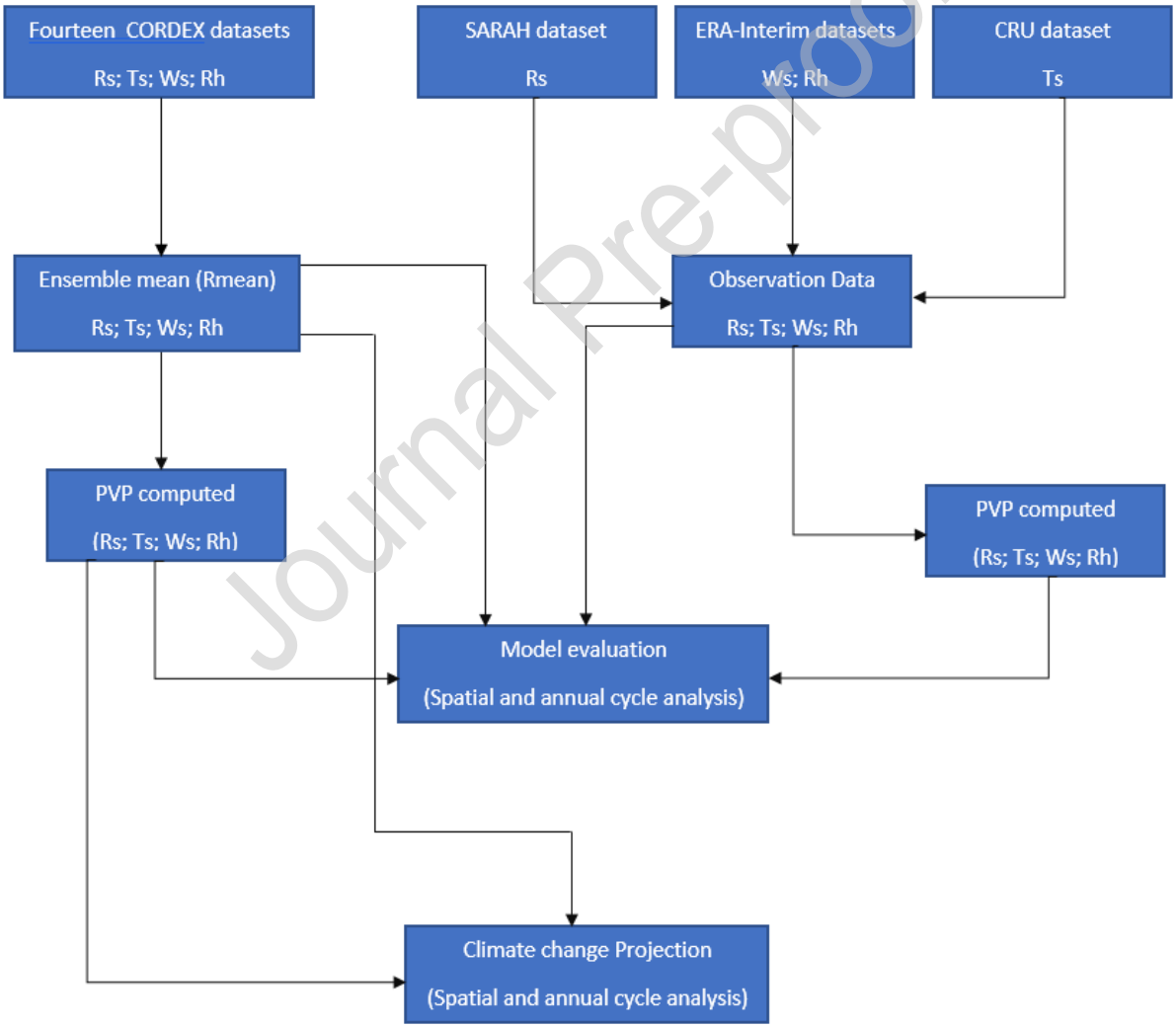

Figure 3: Flow chart of research methodology to characterize the impact of climate change on PV power generation potential over West Africa.

2.3.1 PV power generation potential (PVP)

The PV power generation is defined as the amount of energy received from the sunshine at the Earth's surface and converted into electricity through PV cells, modules and arrays. It results from the PVP multiplied by the nominal PV power installed capacity (in Watts). The PVP describes the performance of the PV cells regarding their nominal power capacity according to the actual ambient conditions and it is dimensionless (Jerez et al., 2015). Besides that, the PVP depends on the solar resource available at the location, the air temperature, wind speed, cloud cover, aerosols, the spectral distribution of incident radiation, the angle of incidence of radiation, and operational efficiencies of system components (Kafka and Miller, 2019). For this study, we use only the solar irradiance (at the plane of the array), the temperature, the wind speed and the relative humidity to quantify the PVP over the study domain. Following Mavromatakis et al (2010), the PVP can be expressed as :

$$PVP(t) = P_r(t).\frac{Rs(t)}{Rs_{STC}} \quad (1)$$

where Rs is the surface-downwelling shortwave radiation at the location site, Rs_{STC} is the solar irradiance of 1000W/m^2 at standard test conditions (STC). $P_r(t)$ is the performance ratio; it accounts for changes of the PV cells efficiency due to changes in their temperature (Jerez et al., 2015) and defined as:

$$P_r(t) = 1 + \gamma.[T_{cell}(t) - T_{STC}] \quad (2)$$

where T_{cell} is the PV cell temperature and T_{STC} is the ambient air temperature at STC i.e. 25 °C. γ is constant and depends on the type of PV cells. In this paper, we use a monocrystalline silicon solar panels for the simulations because it is the most used PV solar technology in West Africa**;** the value of γ is taken as -0.005 °C^{-1} (Jerez et al., 2015). We suppose that the technology will remain the same in the future. Tcell is modelled as a function of Rs, Ws, Ts, and Rh (TamizhMani et al., 2003):

$$T_{cell}(t) = c + c_1.Rs(t) + c_2.Ts(t) + c_3.Ws(t) + c_4.Rh(t) \quad (3)$$

with *c = 1.57°C; c_1 = 0.0289°C/W/m^2; c_2 = 0.961; c_3 = -1.457°C/m/s; and c_4= 0.109°C/Rh%*

where *c, c_1, c_2, c_3 and c_4* are system-specific regression coefficients determined by TamizhMani et al (2003).

We chose this model because it includes the influence of wind speed and relative humidity in calculating the impacts of temperature on PV cells. Other models based their calculations of solar cell temperature on solar irradiance and ambient temperature alone (Crook et al., 2015), meanwhile some studies (Bhattacharya et al., 2014; Kazem et al., 2012) have shown that the solar cell temperature is sensitive to ambient wind speed and relative humidity as well. For instance, Mekhilef et al (2012) showed two scenarios through which humidity can influence PV cell performance: through effect of water vapour particles on solar irradiance and through the humidity ingression to the solar cell enclosure. The authors showed that an increase in relative humidity can reduce the performance of PVP because water droplets on the cell reflect the solar irradiance. On the other hand, an increase in wind speed cools the cells, thereby improving the PV cell efficiency. Hence, choosing the model helps us to obtain a more reliable cell temperature and to compare the contribution of the two additional variables on the cell temperature. Moreover, the model has been developed and evaluated using field measurements of modules (i.e. cell) temperature, ambient temperature, wind speed, wind direction and relative humidity from the weather station. TamizhMani et al (2003) showed that the correlation between the model results and observation is more than 0.9. Jerez et al (2015) have also used the model to project impacts of climate change on PV power generation over Europe.

The Rmean projections in PVP, Rs, Ws and Rh are expressed in relative terms by making the difference between each GWL and the reference period (1971-2000) and then dividing with the historical period of each grid point. However, the projection Ts is expressed in the absolute terms by obtaining the difference between each GWLs and the reference period. All the simulations were compared to the reference datasets before making the climate change projection.

2.3.2 Induced changes in PVP

To compute the contribution of each variable to the projected changes in PVP, we substituted the (2) and (3) into the equation (1) and can be expressed as:

$$PVP(t) = \beta_1.Rs(t) + \beta_2.Rs(t)^2 + \beta_3.Rs(t).Ts(t) + \beta_4.Rs(t).Ws(t) + \beta_5.Rs(t).Rh(t) \quad (4)$$

where $\beta 1 = 1.11715.10^{-3}\,(W/m^2)^{-1}$; $\beta 2 = -1.45.10^{-7}10^{-3}\,(W/m^2)^{-2}$;
$\beta 3 = -4.805.10^{-6}\,(W/m^2.°C)^{-1}$; $\beta 4 = 7.285.10^{-6}\,(W/m^2.m/s)^{-1}$; *and*
$\beta 5 = -5.45.10^{-7}\,(W/m^2.Rh\%)^{-1}$

With the first order of Taylor expansion, the total change in PVP (ΔPVP) due to the contribution of changes in each term in the equation (4) can be expressed as:

$$\Delta PVP = \Delta Rs\_PVP + \Delta Ts\_PVP + \Delta W\_PVP + \Delta Rh\_PVP \quad (5)$$

where : $\Delta Rs\_PVP = \Delta Rs\ (\beta 1 + 2\beta 2.Rs + \beta 3.Ts + \beta 4.Ws + \beta 5.Rh)$;

$\Delta Ts\_PVP = \beta 3.Rs.\Delta Ts$;

$\Delta Ws\_PVP = \beta 4.Rs.\Delta Ws$; and

$\Delta Rh\_PVP = \beta 5.Rs.\Delta Rh$;

So, the total change in ΔPVP due to the contribution of change in temperature (ΔTs_PVP) is obtained by:

$$\Delta PVP = \Delta Ts\_PVP \quad (6)$$

A similar analysis can be used to isolate the other terms from Equation (5). Table 1 summarized all the parameters used; with their meaning and unit.

Table.1 Different parameters with their meaning and units used in this study

Parameter	Meaning	Unit
Rs	Solar irradiance	W/m^2
Ts	Air temperature	$°C$
Ws	Surface wind speed	m/s
Rh	Relative humidity	%
PVP	PV power generation potential	dimensionless
ΔRs	Change in solar irradiance	W/m^2
ΔTs	Change in air temperature	$°C$
ΔWs	Change in surface wind speed	m/s
ΔRh	Change in relative humidity	%
ΔPVP	Change in PV power generation potential	dimensionless
ΔRs_PVP	The total ΔPVP due to the contribution of ΔRs	dimensionless
ΔTs_PVP	The total ΔPVP due to the contribution of ΔTs	dimensionless
ΔWs_PVP	The total ΔPVP due to the contribution of ΔWs	dimensionless
ΔRh_PVP	The total ΔPVP due to the contribution of ΔRh	dimensionless

3. Results and discussions

3.1 Model evaluation

The Rmean reproduces well the spatial distribution of solar irradiance (Rs), surface temperature (Ts), wind speed (Ws), and relative humidity (Rh) over West Africa (Fig. 4). For each variable, the spatial correlation between the simulated and observation annual mean is high (significant at 95% of confidence level), ranging from 0.90 in Ts to 0.99 in Rh. Furthermore, the Rmean exhibits a low spatial mean bias deviation (MBD), varying from -2.6% in Rs to -15% in Rh with a low root mean square deviation (RMSD) over the region. The simulations capture the latitudinal variation of variables. In agreement with observation, the Rmean simulate the minimum Rs, Ts and Ws over the Guinea coast and maximum values over the Sahel zone. While the minimum Rs (about 160 W/m^2) over the Guinea zone can be attributed to cloudiness from deep convection and land-sea-breeze that may intercept the incoming solar radiation (Knippertz et al., 2011), the maximum Rs (about 300 W/m^2) over the Sahel zone may be due to cloud free-conditions over the zone for most of the year (Parker and Diop-Kane, 2017). Nevertheless, the lower Ts over Guinea (compared to that over the Sahel zone) may be due to the lower Rs and more vegetation cover (i.e. more evapotranspiration induced cooling) over the zone. The weaker Ws over Guinea (compared to that over the Sahel) may be due to the stronger frictional drag on the monsoon flow over the zone. The simulation and observation agree that, in contrast to Rs, Ts and Ws, a maximum Rh (> 66%) is in the Guinea zone and a minimum Rh (< 34%) in the Sahel zone. The maximum Rh over Guinea is because the moisture laden monsoon air is advected into the sub-continent through the Guinean zone, and the monsoon flow loses some of its moisture (through rainfall) before reaching the Sahel zones.

Despite the good performance of the Rmean (in reference to the observation), there are some notable biases in the simulation (Fig. 4). For instance, the Rmean underestimates the Rs over most part of West Africa (by up to 20 W/m^2 along the Guinea coast and the eastern part of the Sahel zone) and overestimates it over the western Sahel (by up to 10 W/m^2) (Fig. 4b). This bias suggests that the RCMs overestimate the cloudiness over the Guinea coast and underestimate it over the western Sahel. However, the largest negative biases in the Rs are located over the mountainous areas (like the Jos Plateau in Nigeria and the Fouta Djallon mountain in Guinea), suggesting that the RCMs may be too active in simulating orographic cloud (Aguilar et al., 2010), or in triggering deep convection over the mountains. Several studies have shown that cloud representation is still

a major challenge in climate models (Tang et al., 2018; Palmer, 2016; Solomon et al., 2009). Nevertheless, the discrepancies between the simulated and observed Rs might also be explained by shortcomings in the satellite observation that have been reported in previous studies (Amillo et al., 2018; Urraca et al., 2017; Riihelä et al., 2015). While the RCMs overestimate Ws over the Guinea and Savannah zones and underestimate it over the Sahel region (Fig. 4c), they underestimate Ts and Rh over the entire West Africa. The largest Ts bias is located in the Sahel zone and the lowest in the Guinea and Savannah zones. The opposite is the case for Rh bias.

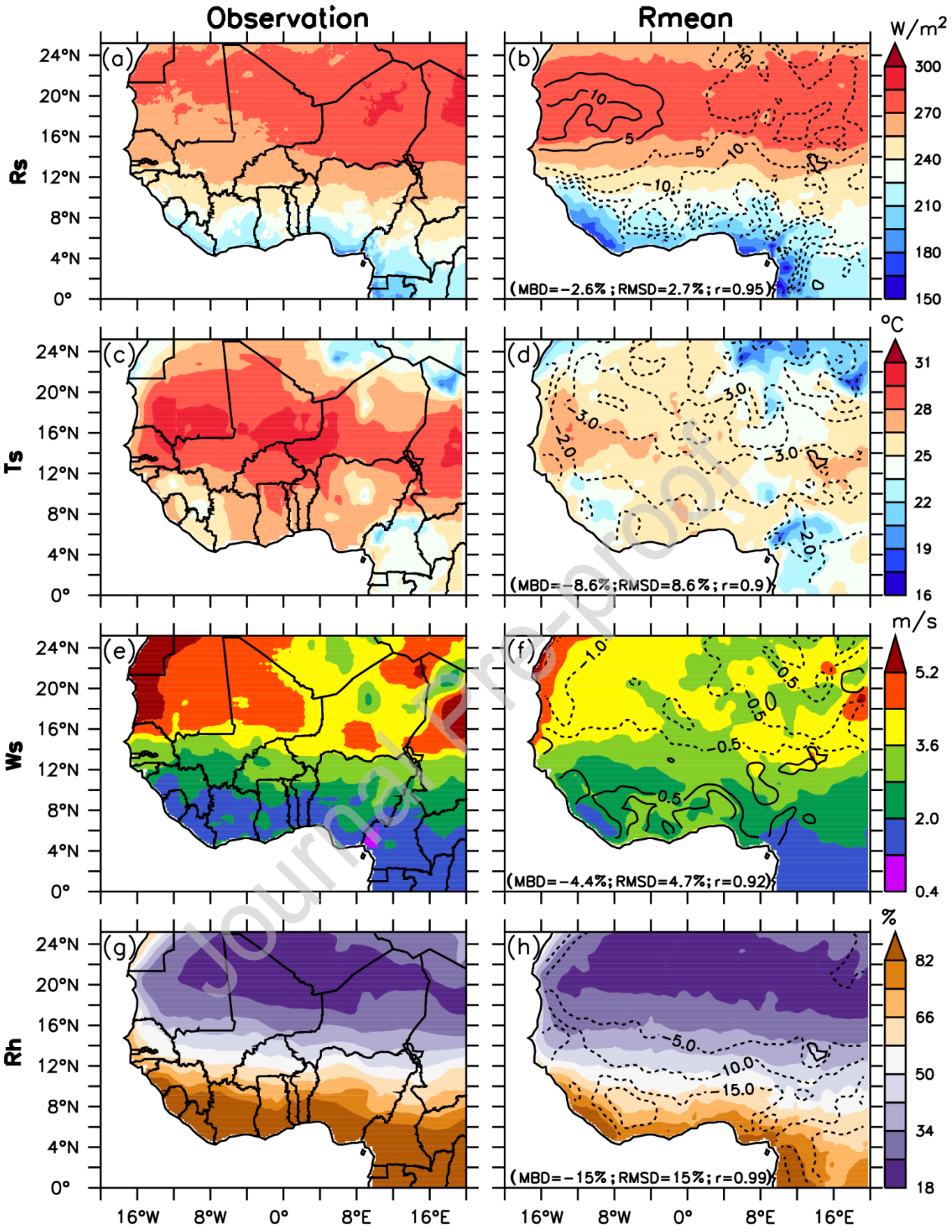

Figure 4: The spatial distribution of the annual averages of solar irradiance (Rs), surface temperature (Ts), surface wind speed (Ws) and relative humidity (Rh) as observed (left column) and simulated (Rmean; right column) over West Africa. The correlation (r), mean bias deviation (MBD) and root mean square deviation (RMSD) between the observed and simulated fields are indicated in the brackets, while the simulation

biases are depicted with contours. All the correlations are statistically significant at 95% confidence interval.

Figure (5) shows that the RCMs (Rmean) replicate the observed annual cycle of the variables (Rs, Ts, Ws, and Rh) over each climate zone. The monthly correlation between the simulated and observed cycle is strong ($r > 0.7$) and significant (at 95% confidence level) for all the variables. In addition, the performance of Rmean varies with different variables and over different zones as well. The Ws shows a higher RMSD of 30% over the Guinea zone while the Rs shows the lowest RMSD of 4.9% over the Sahel zone. However, the RCMs captures the maxima and the minima of the Rs, Ts, Ws and Rh over each zone, although with different magnitude. Over the Guinea zone, in agreement with observation, the Rmean simulates the Rs and Ts maxima with Rh minimum in the dry season December–February, before the arrival of the moist monsoon flow (Sylla et al., 2015) and shows Rs and Ts minima and Rh maximum in peak wet season (August, during the monsoon flow). However, in general, the MBD shows that the Rmean underestimate the observed value of the variables over the different zones. For instance, the Rmean underestimates the observed Rs minimum (by more than 50 W/m^2) and underestimates Rh throughout the year (by about 20%) except in the Sahel zone, and overestimates the wind speed in all months (by about 1 m/s) over the Sahel at less than 0.5 m/s over the Guinea and Savannah zones. The annual cycles of these variables over the Savannah and Sahel zones are similar to those over the Guinea zone, except that both observation and Rmean indicate that Rs and Ts maxima with Rh minima over the Savannah zone occur a month later than their counterparts over the Guinea zone, and those over the Sahel zone also occur a month later than their counterparts over the Savannah zone. This is consistent with the northward movement of the pre-monsoon condition over West Africa (Cornforth, 2012). The magnitude of the Rmean biases over the Savannah-Sahel zones is also comparable to those over the Guinea coast. These results agree with those in previous studies (e.g. Abdullahi et al., 2017; Gilani et al., 2011) that showed that high temperature goes with high solar radiation while high relative humidity reduces the solar radiation.

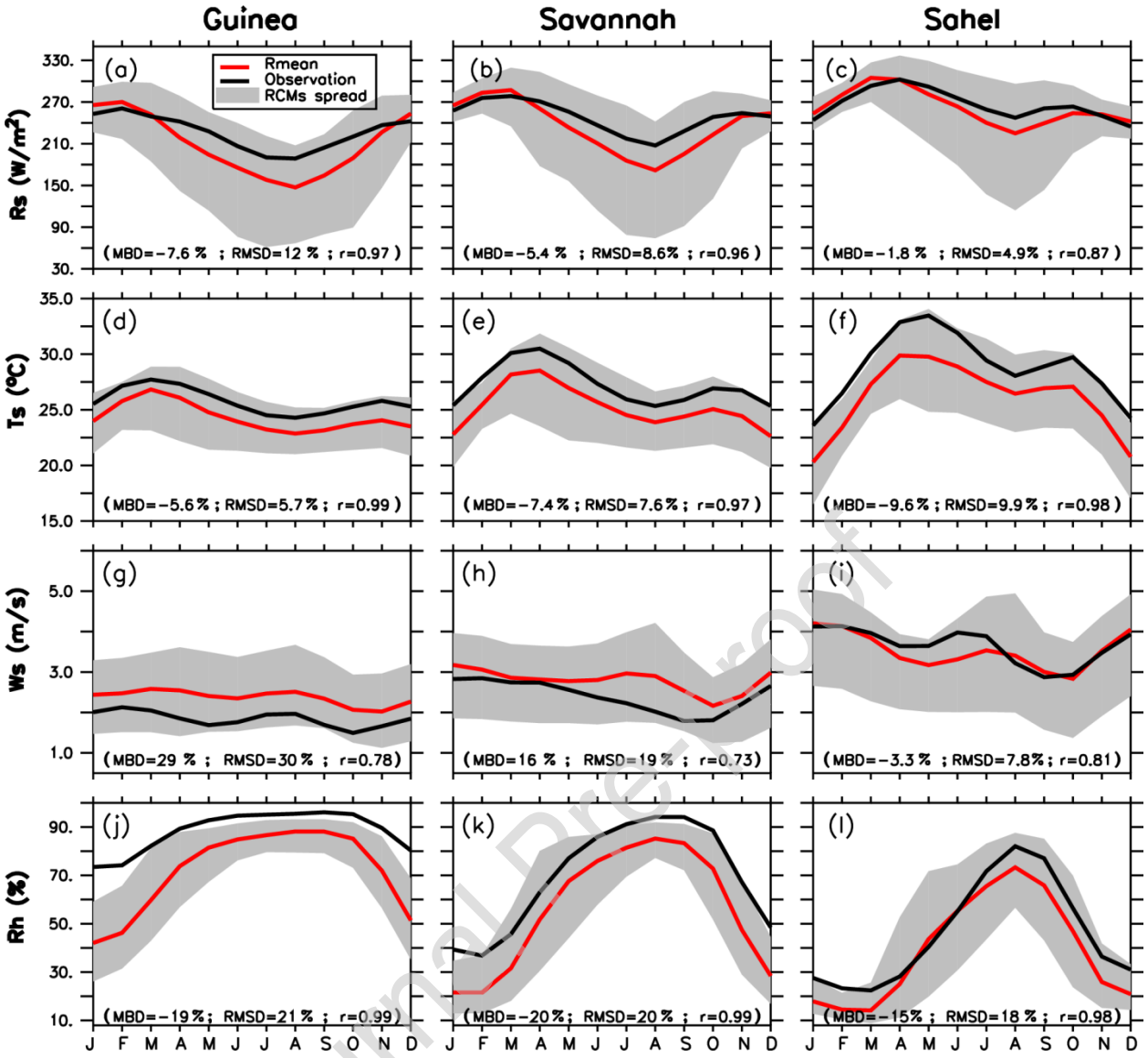

Figure 5: The observed and simulated annual cycle of solar irradiance (Rs), surface temperature (Ts), surface wind speed (Ws) and relative humidity (Rh) over the three West African zones (Guinea, Savannah and Sahel). The simulation spread is in grey while the simulation mean (Rmean) and observed values are in black and red lines, respectively. The correlation (r), mean bias deviation (MBD) and root mean square deviation (RMSD) between the observation and Rmean is indicated in the bracket. The asterisk (*) indicates the correlations that are statistically significant (at 95% confidence level).

The Rmean also replicates the spatial distribution of PVP over West Africa, with a high correlation value (r=0.95) and a low RMSD (5.6%; Fig. 6a & b). In agreement with observation, Rmean locates the highest PVP over the Sahel region (19.53-28.75%) and the lowest over the Guinea zone (13.05-24.75%). The pattern mostly follows the spatial distribution of Rs, and to an extent, that of Ts. The major shortcoming in the spatial distribution of the simulated PVP is the positive bias (about 1%) over the western part of the Sahel zone and the negative bias over the western part of

the Guinea zone (about 0.5%). Nonetheless, the Rmean underestimates the observed PVP over West Africa with a value MBD of -5.5%. Over the zones (Guinea, Savannah, and Sahel), the observed annual cycle of PVP mimics that of Rs, showing the highest PVP (24.89%, 27.15%, 29.28%, respectively) in February when clear sky gives room for maximum Rs and the lowest values (24.89%, 27.15%, 29.28%, respectively in August when the presence of clouds reduces the Rs to the minimum). The Rmean realistically reproduces this annual cycle, but with a larger amplitude than observed; while it overestimates the maximum values, it underestimates the minimum values. These biases are consistent with those in the simulated Rs. Nevertheless, the simulated annual mean of PVP over the country is in good agreement with the observation. While the observed values fall within the interquartile of the model spread over most of the countries, all the RCMs underestimate the mean observed of the PVP over Liberia, Serra-Leone and Guinea-Bissau (Fig. 6f). This may due to the different biases in the simulated variables used in computing the PVP. However, the simulations and the observation agree that the highest PVP is in Niamey (25.98%) and the lowest value is in The Gambia (14.85%). The good agreement between the simulations and observation on the spatio-temporal variation of Rs, Ts, Ws and PVP suggest that the simulations capture the necessary atmospheric processes (e.g. monsoon systems) that control PVP variation over West Africa.

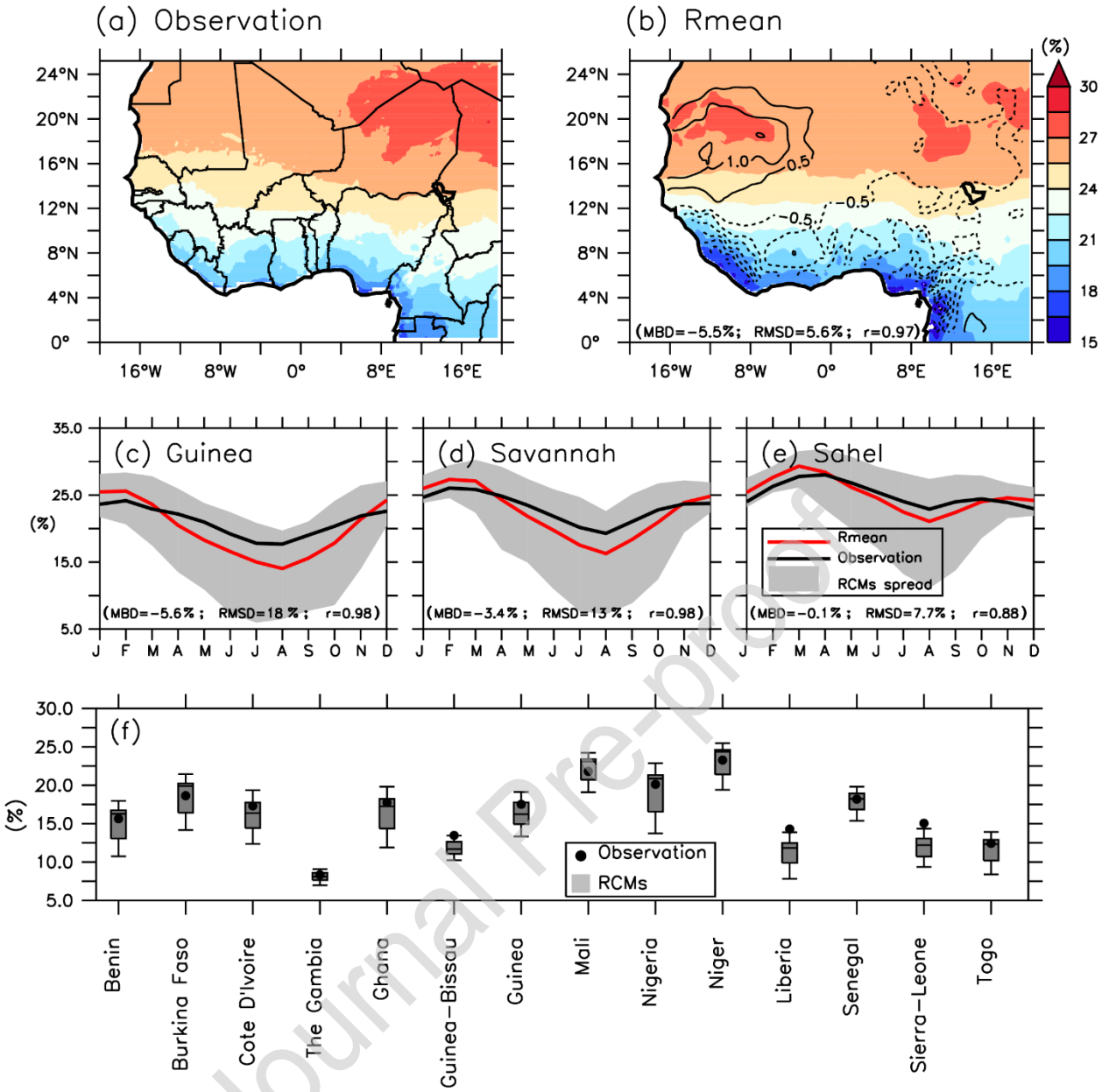

Figure 6: The climatology of PV power generation potential during the reference period (1971-2000) as observed and simulated. The contours in panel (b) show the simulation bias. The panels (c-d-e) show the spread of the simulated PV power generation potential over the three zones (Guinea, Savannah, and Sahel). The correlation (r), mean bias deviation (MBD) and root mean square deviation (RMSD) between the observation and Rmean is indicated in the bracket. Panel (f) shows the same over the countries. Each boxplot indicates the minimum, 1st quartile, median, 3rd quartile, and maximum of RCMs.

3.2 Climate change projection

3.2.1 Projected changes in PVP and climate variables.

The simulation ensemble projects a decrease in the PVP over West Africa, except along the coastal and mountainous areas where it projects an increase (Fig 7). These changes are statistically

significant at 95% over the whole region under the GWLs. However, the magnitude of the change varies over the region and increases non-linearly with increasing GWLs (Fig 7a-d). At GWL1.5, the decrease is about 0.72% north of 16^{o}N and less than 0.72% south of this latitude. In general, the PVP decreases by 0.5% between GWL1.5 and GWL2.0 but by 0.4% between GWL2.0 and GWL2.5 (Fig 7). So, at GWL2.5, a decrease of about -1.5% is projected north of 16^{o}N and about 1.35% is projected south of this latitude. The result is consistent with previous studies that have shown that climate change may reduce the PV power output over West Africa. For example, Huber et al. (2016) projected a general decrease in PVP over West Africa. They used an ECHAM4 (GCM) coupled with the aerosol-climate model for the future period of 2035-2039 compared to the past period (1995-1999). Using eight regional climate models (CORDEX), Bazyomo et al. (2016) also projected a decrease of PVP over the West African countries.

The projected changes in PVP (hereafter, ΔPVP) can be explained by the corresponding changes the four climate variables (hereafter, ΔRs, ΔTs, ΔWs and ΔRh; Fig. 7). Among the four, ΔRs has the highest spatial correlation ($r > 0.93$) with ΔPVP (Fig. 6e-h). The spatial distribution of ΔTs also has a high but negative spatial correlation ($|r| \geq 0.82$) with ΔPVP, although the magnitude of the correlation reduces with GWLs (Fig. 7i-l). However, the strong negative spatial correlation between the changes in Ts and PVP indicates that an increase in Ts contributes to the projected decrease in PVP. This is consistent with previous studies that report that an increase in temperature leads to a decrease in PVP (Wild et al., 2015; Jerez et al., 2015; Dubey et al., 2013; Fesharaki et al., 2011). Hence, in addition to the influence of solar dimming, the maximum increase in Ts over the Sahel could also induce the maximum decrease in PVP over the zone. In contrast to ΔRs and ΔTs, ΔWs and ΔRh are poorly correlated with ΔPVP (Fig. 7). The correlation between ΔWs and ΔPVP ranges from -0.18 (at GWL1.5) to 0.47 (at GWL2.5), while the correlation between ΔRh and ΔPVP ranges from -0.02 (at GWL2.0) to 0.21 (at GWL3.0). Nonetheless, ΔWs and ΔRh are only significant (at 95% confidence level) at GWL2.0 and GWL3.0, where an increase in Ws (maximum: 4.7%) and a decrease in Rh (maximum: 6.4%) are projected over the Sahel. The direction of changes in Ws and Rh are not consistent with that of PVP, in that, the projected increase in Ws and decrease in Rh over the Sahel zone would increase the PVP. This suggests that the influence of change Rs and Ts dominate the projected change in PVP.

The Rmean project a general decrease in Rs and Rh while an increase in Ts and Ws over the region. As in ΔPVP, ΔRs generally decreases (up to 1%) over West Africa with a little increase along the

coastal zones and mountainous areas at all the GWLs; at GWL3.0, the maximum decrease is located in the Guinean zone (2.02%), the minimum decrease is in the Sahel zone (1.43%). Counterintuitively, global warming may reduce solar irradiance over West Africa. This reduction (known as solar dimming) is due to the feedback of the global warming change Rs through in cloud cover and aerosols. For instance, some studies have projected an increase in precipitation and cloud cover over the Guinea zone (Sylla et al., 2010) under the warmer climate and a higher concentration of aerosols over the Sahel (Touré et al., 2012). On the other hand, an increase in Ts over West Africa is projected with the increase GWLs, but the regional warming rate is higher than the global rate, especially at north 12^{o}N, where warming is more than 1.2^{o}C per 1^{o}C GWL; the rate is even more at east Sahel (> 1.3^{o}C per 1^{o}C GWL). This pattern is consistent with previous studies (e.g., Sylla et al., 2016; Abiodun et al., 2012) that attributed the lowest warming rate along the coast to the cooling effect of the monsoon air from the ocean. The cooling effect, which decreases inland, may be weak or absent over the Sahel zone. Nonetheless, the increase in Ws can be attributed to the projected stronger temperature gradient over West Africa (i.e. Abiodun et al., 2012; Sawadogo et al., 2019), while the decrease in Rh can be due to high saturated mixing ratio in the projected warmer climate (i.e. Abiodun et al., 2012).

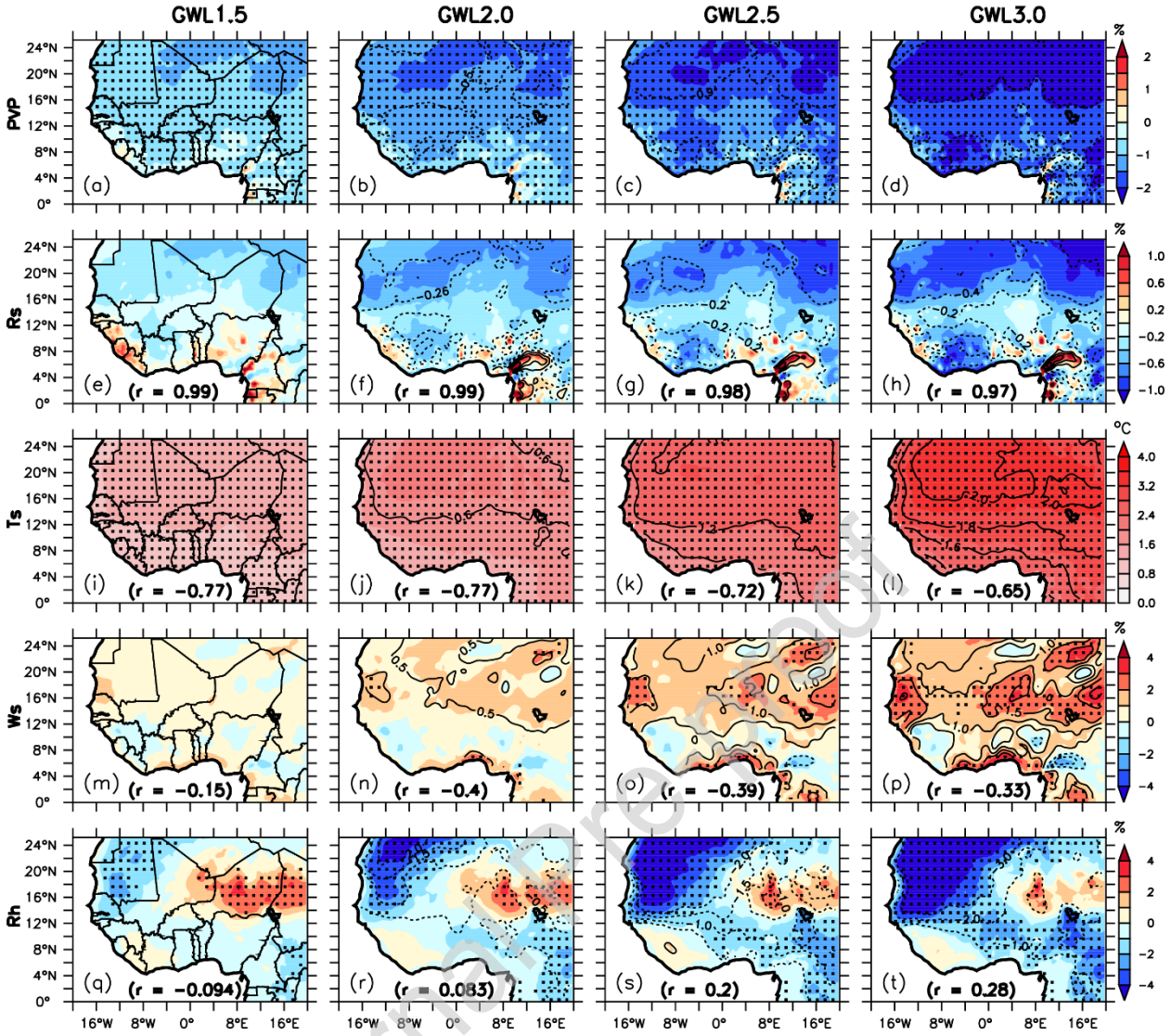

Figure 7: Projected changes in PV power generation potential (PVP) of the model ensemble mean, solar irradiance (Rs), surface temperature (Ts), wind speed (Ws), and relative humidity (Rh) over West Africa under the four global levels (GWL1.5, GWL2.0, GWL2.5, and GWL3.0). The area where the changes are statistically significant (at 95% confidence level) are indicated with dots. The contour lines indicate the difference between the GWL15 and each corresponding GWLs. The correlation between the PVP pattern and other variables is shown in brackets.

Figure (8) reveals that the projected decrease in PVP (i.e. negative ΔPVP) over West Africa does not occur throughout the year. A positive ΔPVP is projected in April to May over the Guinea zone, in May and July over the Savannah and the Sahel zone (Fig. 8a - 8c). However, while the negative ΔPVP can be as much as -2.8% (in November–January; Fig. 8c), the maximum positive ΔPVP is about 2.41% over the Sahel and the Savannah zones (in July; Fig. 8c). The month variation of ΔPVP is better coupled with ΔRs, ΔWs and ΔRh than with ΔTs (Fig. 8). This implies that the impacts of the regional warming on PV over each zone are minimal in months when the monsoon

system arrives over the zones. The figure shows that these periods are associated with positive ΔRs and ΔWs and negative ΔRh. The negative ΔRh suggests drier condition and less cloudiness because the warmer atmosphere would require more moisture to reach saturation and produce clouds. And the positive ΔRs is consistent with less cloudiness as a decrease in cloudiness will allow more insolation to reach the surface. All these changes would tend to induce a positive ΔPVP during this period. Hence, the arrival of the monsoon system plays a crucial role in modulating the impact of global warming on the seasonal variation distribution of ΔPVP.

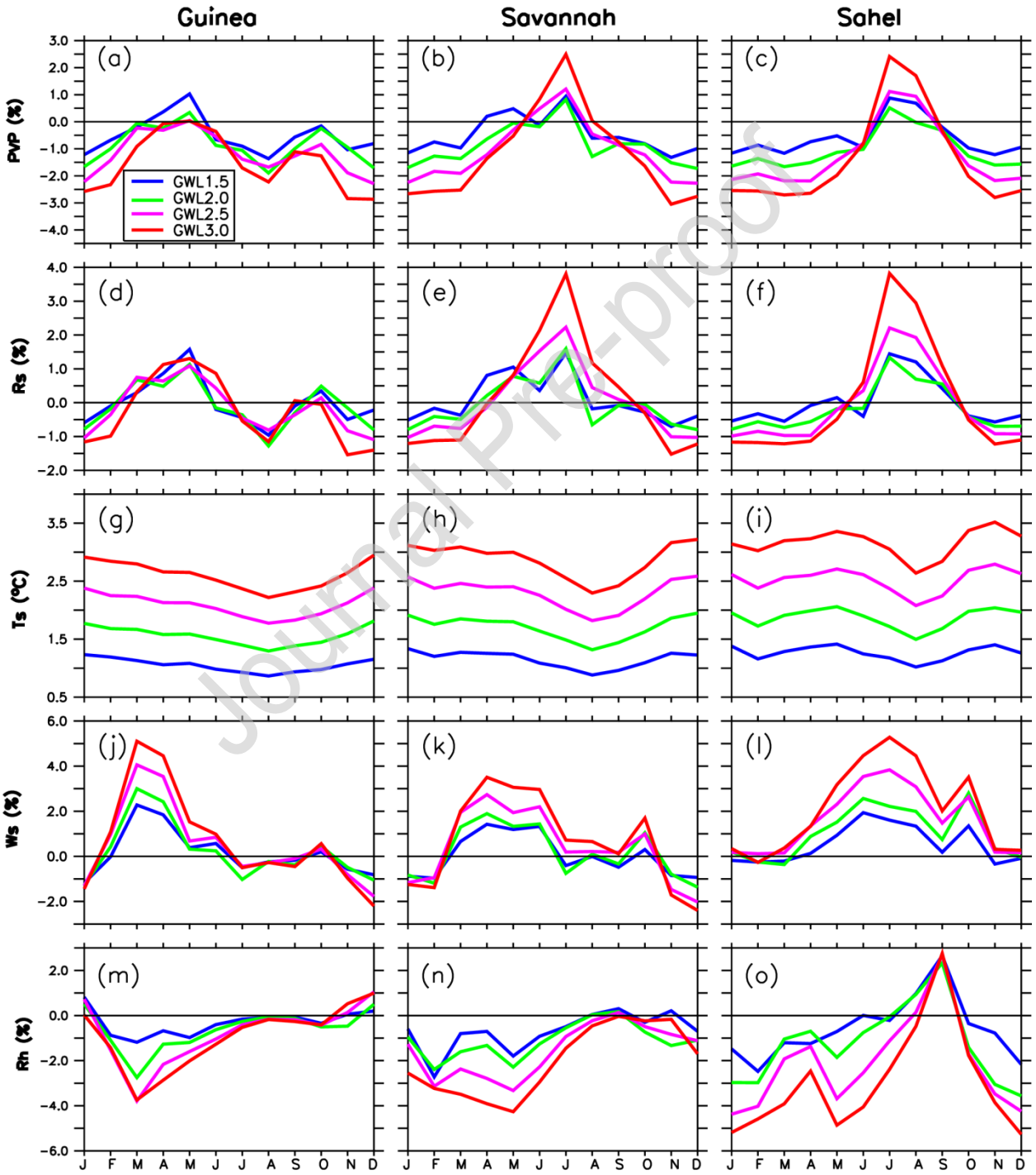

Figure 8: Projected changes of the model ensemble mean in the annual cycle distribution over different West African zones under the four GWLs (GWL1.5, GWL2.0, GWL2.5, and GWL3.0): (a-c) shows for the PV power generation potential (PVP); (d-f) for the solar radiation (Rs); (g-i) for the air temperature (Ts); (i-k) for the Ws and (i-n) for the Rh

3.2.2 Projected changes in PVP over West African countries

The simulation ensemble projects a decrease in PVP over all the selected countries (Fig. 9). However, the level of agreement among the simulations on the projection (which is a measure of the robustness of the projections) varies over the countries. For example, at GWL1.5, while less than 75% of the simulations agree on the decrease in Sierra-Leone and Liberia, more than 75% of the simulations agree on it over other countries. The discrepancy among the simulations on the projection may be attributed to the differences in the simulation configuration (Jerez et al., 2018; Giorgi, 2010). Nonetheless, the robustness of the projection over all the countries increases with increasing GWLs, such that, at GWL3.0, more than 75% agree on the decrease over all the countries. The magnitude of the projected decrease also varies over the countries. Among the countries, Niger is projected to experience the largest decrease (about -2.13% at GWL1.5 and about -3.59% at GWL3.0). This is coherent with the study of Bazyomo et al. (2016) that indicated Niger to have the highest decrease in West Africa by 2045. However, the magnitude of the decrease of PVP differs with the results of Bazyomo et al (2016) where the maximum decrease of the mean trend is about 0.032% /year or 1.28% for the period of 2006-2045. In general, the results of Bazyomo et al. (2016) in the PVP projection are lower than our results.

The magnitude of the decrease in PVP projected over the West African countries is much lower than the one projected in Europe and similar to some region in the world. For instance, using EURO-CORDEX simulations, Jerez et al (2015) projected -14% decrease over some Northern European countries. In addition, with the HadGEM1, California (~ -2%), Nevada (~ -3.5%), Algeria (~ -1%), Saudi Arabia (~ -5%) and Australia (~ -0.5%) may experience a decrease in PVP. On the other hand, some countries like China, Spain, and Germany may know an increase in the PVP (Crook et al., 2011). This suggests that the impact of climate change on PVP varies according to the regions with different magnitudes. Even if our results show a similar magnitude in the change of the PVP compared to other regions, the results of this study should be taken with care due to the model errors and uncertainties in the projection. However, with the ongoing project over the region at the large scale for electricity production, decision-makers should take into account

the future decrease of the PVP in their agenda. In addition, the sector of solar energy may be driven by the joint economic impact of climate change and technology development. To compensate the losses due to the impact of climate change, we need to install more solar plants or even to go for higher efficiency cost-effective solar cells that may allow to use the same land and infrastructure, by replacing the modules that have 15-20 years life expectancy.

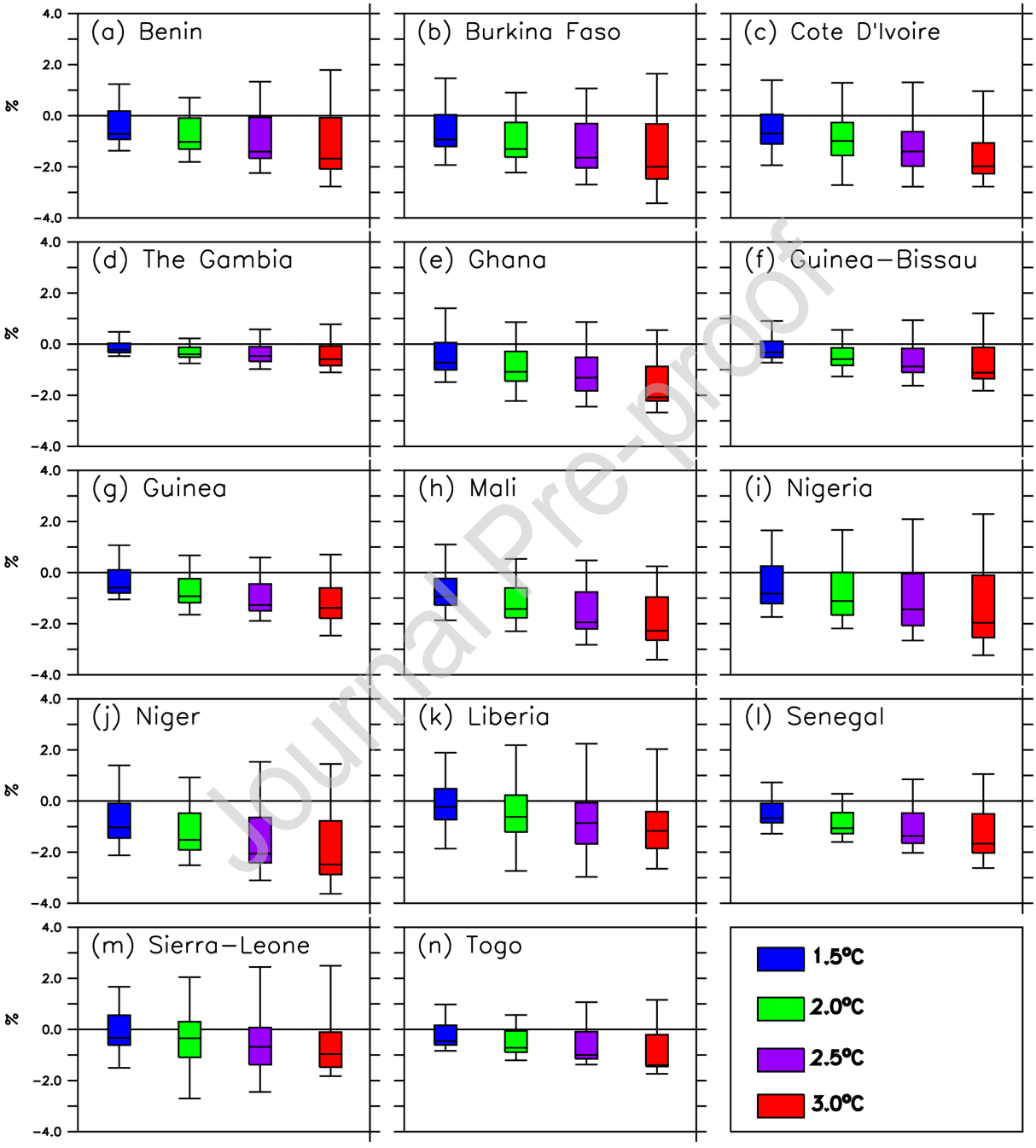

Figure 9: Projection of annual mean PV power generation potential (PVP) over the West African countries under the four GWLs (GWL1.5, GWL2.0, GWL2.5, and GWL3.0. Each boxplot indicates the minimum, 1st quartile, median, 3rd quartile, and maximum of the RCMs.

3.2.3 Total change in PVP due to the contribution of Rs, Ts, Ws and Rh

The spatial distribution of the total change in PVP (ΔPVP) due to the contribution of change in temperature (ΔTs_PVP) exhibits the largest contribution over West Africa (Fig.10 e-h). This contribution increases as the warming level increases. Moreover, at all warming level, the high magnitude of the contribution is in the Sahel region, whereas low magnitude in the Guinea zone. For instance, over the Sahel the GWL1.5 (-0.632%), GWL2.0 (-0.93%), GWL2.5(-1.26%) and GWL3.0 (-1.58%) is higher than the GWL15 (-0.53%), GWL2.0 (-0.79%), GWL2.5 (-1.06%) and GWL3.0 (-1.32%) over the Guinea zone. This study reveals that as the global warming level increases, the increase in local temperature over the region contributes to decreasing the PVP. The results of this study are in lines with previous studies showing that the increase in temperature drops the efficiency of the solar cells; hence the PVP (Fesharaki et al., 2011; Radziemska, 2003). It why some studies advocate to reduce the vulnerability of the PV cells performance to the ambient temperature (Jerez et al., 2015; Patt et al., 2013). The general decrease in Rs also contributes to the total change in PVP over the region. The ΔPVP due to the contribution of change in solar irradiance (ΔRs_PVP) exhibits a positive value along the coastal area and mountainous zones and negative value elsewhere (Fig.10 a-d). Also, the contribution of ΔRs_PVP increases with the warming level. For example, over the Sahel zone, the ΔRs_PVP contributes about -0.24% under GWL1.5 while -0.54% under GWL3.0. On other hands, the contribution of ΔWs_PVP (Fig.10 i-l) and ΔRh_PVP (Fig.10 m-p) have an insignificant effect on the total change the PVP under the various warming level. This could be explained either by the small contribution of Ws and Rh used in equation 3 or to the small changes of the projection of both variables. Overall, this suggests that the total change in PVP may come from the change in Rs and Ts but mostly to the change of Ts.

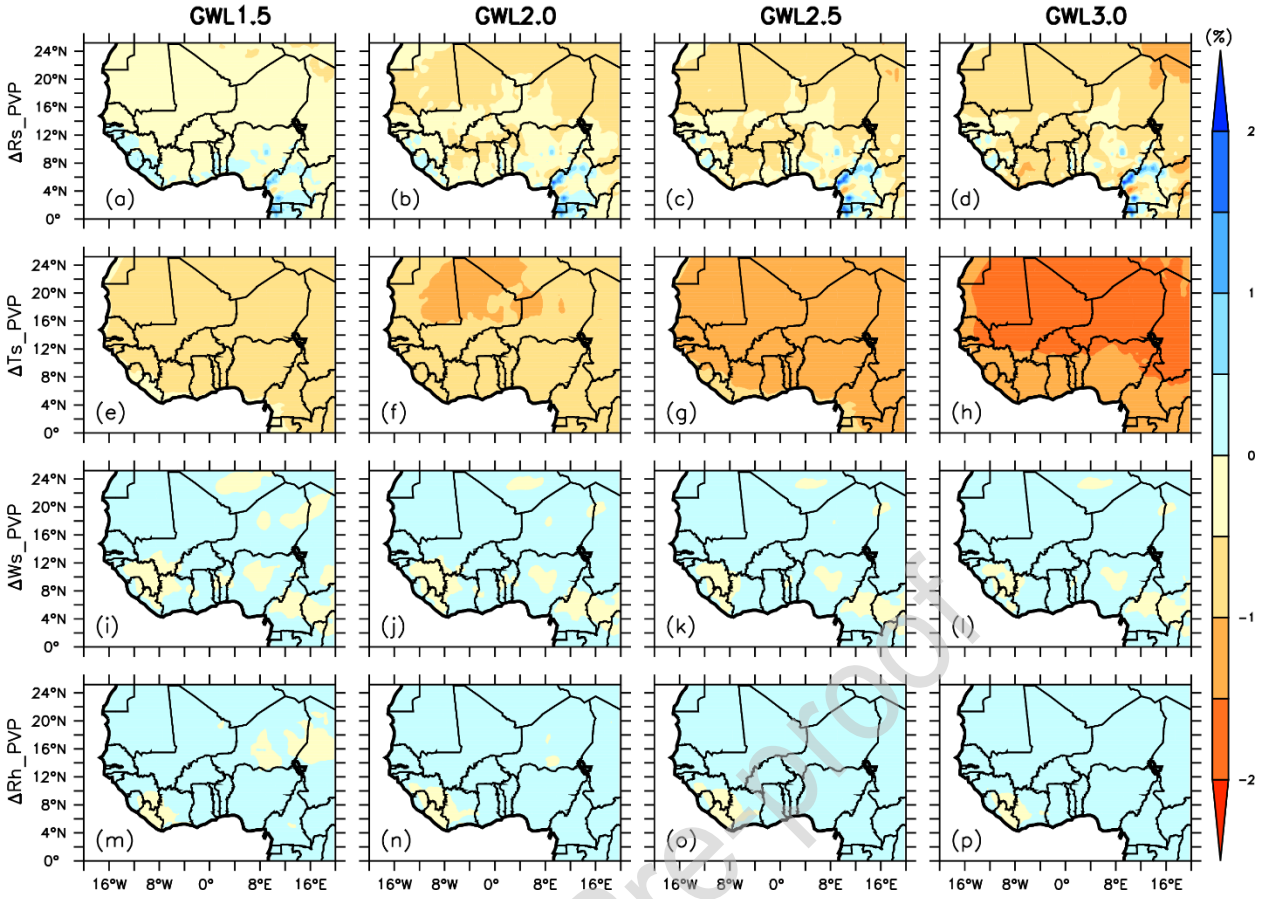

Figure 10: Projection of ensemble mean of the total change in PVP due to the contribution: change in solar irradiance (ΔRs_PVP) (a-d); change in temperature (ΔTs_PVP) (e-h); change in wind speed (ΔWs_PVP) (i-l) and change in relative humidity (ΔRh_PVP) (m-p) over the West African countries under the four GWLs (GWL1.5, GWL2.0, GWL2.5, and GWL3.0

Among the seven components of ΔPVP in Equation (5), ΔRs_PVP and ΔTs_PVP have the largest contributions to ΔPVP (Fig.11). The contributions from other components (ΔWs_PVP, ΔRh_PVP) are negligible. That is why their plots are overlaid and close to zero. However, the characteristics of ΔRs_PVP and ΔTs_PVP differ. For instance, in the annual cycles, ΔRs_PVP features positive values in some seasons and negative in others, while ΔTs_PVP features negative values throughout the year. So, the contributions of ΔTs_PVP and ΔRs_PVP to ΔPVP are additive in some seasons but opposite in other seasons. In addition, while the magnitude of ΔRs_PVP is virtually invariant with the increasing GWLs, that of ΔTs_PVP increases with the increasing of GWLs. At GWL1.5, the negative contribution of ΔTs_PVP to ΔPVP is lower than the positive contribution from ΔRs_PVP in some seasons, making ΔPVP to be positive. But, at GWL3.0, the negative contribution overwhelms the positive contribution of ΔRs_PVP throughout the year.

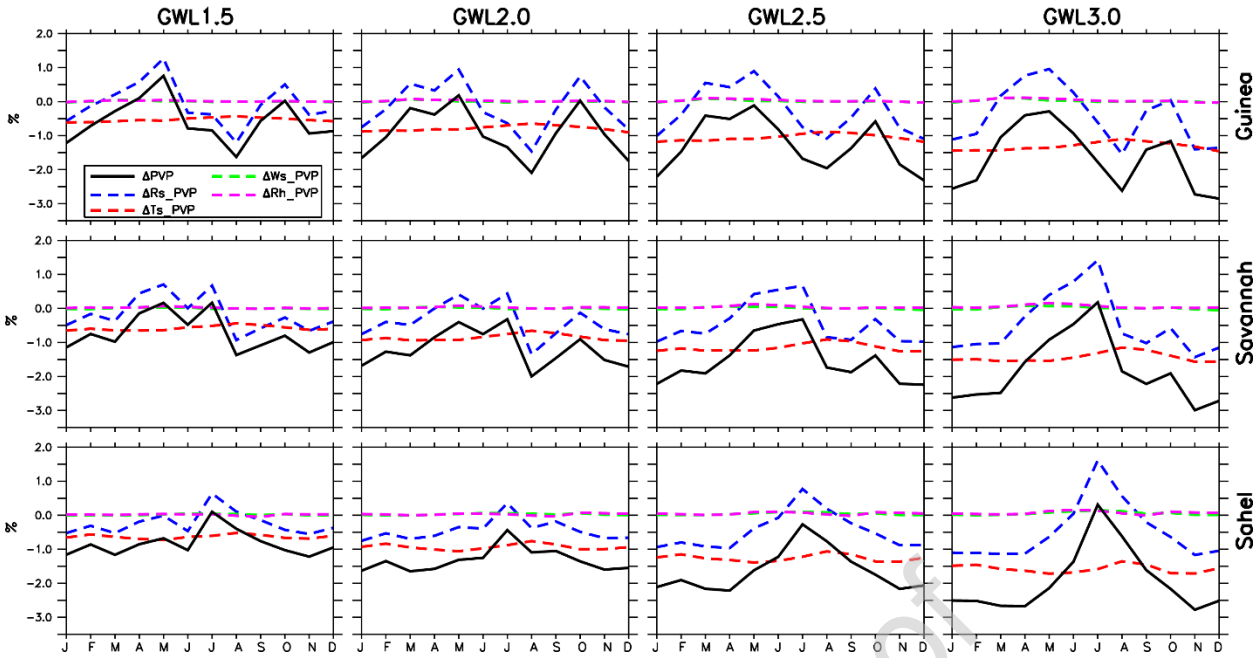

Figure 11: Projected annual cycle of the contribution of each term to the projected change PV power generation potential over different West African zones and under various global warming levels.

4. Conclusion

To understand the potential impacts of climate change on the PVP over West Africa, we have analysed 14 RCM simulations from the CORDEX dataset at specific global warming levels under the RCP8.5 climate scenario. The capability of the simulations to reproduce climate variables (i.e. solar irradiance, ambient air temperature, surface wind speed, and relative humidity) which influence the efficiency of solar panel cells was evaluated by comparing the simulations with observations (SARAH and CRU) and reanalysis data. The projected changes in PVP (i.e. ΔPVP) and climate variables (i.e. ΔRs, ΔTs, ΔWs and ΔRh) were obtained at four GWLs (1.5 °C, 2.2 °C, 2.5 °C, 3.0 °C), and the spatio-temporal relationship between the ΔPVP and of ΔRs, ΔTs, ΔWs and ΔRh was examined. The relative contribution of each component in the equation (5) to ΔPVP was analysed. The results of the study can be summarized as follow:

- The CORDEX simulation ensemble mean reproduces well the spatial distribution of climate variable (Rs, Ts, Ws and Rh) and PVP over West Africa, but it underestimates Rs over most part of West Africa over the eastern Sahel and overestimates it over the western Sahel.
- The ensemble mean captures the annual cycle of the climate variables and PVP over each climate zone shown. For all the variables, the simulation ensemble spread encloses the

observed curves. In agreement with observation, the simulations show that the seasonal cycle of PVP is controlled by the monsoon system.

- The CORDEX simulations projected a decrease in PVP over the whole of West Africa and indicate the magnitude of the increases with the increasing GWLs. The decrease is mainly due to projected solar dimming and increased regional temperature following global warming. However, the spatial distribution of ΔPVP is more influenced by ΔTs than by ΔRs.
- The annual cycle of ΔPVP shows an increase (or least decrease) in PVP during the arrival of the monsoon system over each zone because, following the global warming, the onset of the monsoon system features stronger wind, drier condition, less cloudiness, and more radiation. The budget of ΔPVP shows that during the arrival of the monsoon system, the magnitude of ΔRs_PVP (positive) is more that of ΔTs_PVP (negative), especially at GWL1.5
- More than 75% of the simulations agree on the decrease in PVP over most of the selected countries, especially at GWL3.0. A maximum decrease is projected over Niger.

The results of this paper can be improved in many ways. For instance, given that the PVP projection over West Africa is very sensitive to the uptake and removal of atmospheric dust by dry and wet convective systems (respectively), high-resolution simulations could give a better representation of the convections and their vertical transport of atmospheric dust. In addition, simulations that account for moist chemistry in the clouds may also give a better representation of the chemical processes in the clouds. Studies (Zang et al., 2016; Jantsch et al., 1991) have shown that the tilting angle of the solar panel influences PV efficiency. This was not accounted for in the present study. So, incorporating such factors into future studies can improve the robustness of the PVP projection. Furthermore, the focus of our study has been on the impact of climate change on PV, but there are other solar panel technologies. So, understanding the impacts of climate change on other technology, like concentrated solar power (CSP), will help put the results into a better perspective and provide a guide for technology with the least climate change impacts. Finally, the model biases (seen in reference climate simulation) may impact the future projections and produce uncertainty in the projection. Understanding how to identify and reduce the influence model biases in future climate projections requires further investigation. Nevertheless, the present study has shown that global warming may reduce the PVP over West Africa in the future, although the projected maximum decrease is less than 3.8%.

Acknowledgements

Funding for this study was provided by the German Ministry for Education and Research (BMBF) through the West African Science Service Center on Climate Change and Adapted Land Use (WASCAL) and by the South African National Research Foundation (NRF). We thank the CORDEX project for giving access to the simulation data, and ECMWF for providing the reanalysis data. The computing facilities were provided by the Climate System Analysis Group (CSAG) at University of Cape Town (UCT, South Africa) and the Computation Centre for High Performance Computing (CHPC, South Africa). The authors thank the three anonymous reviewers for their comments and suggestions to improve the quality of the paper.

References

Abdullahi, S. A., Abdul, M., & Joshua, and A. (2017). Impacts of Relative Humidity and Mean Air Temperature on Global Solar Radiations of Ikeja, Lagos, Nigeria. *International Journal of Scientific and Research Publications*, *7*(2), 315–319.

Abiodun, B. J., Adeyewa, Z. D., Oguntunde, P. G., Salami, A. T., & Ajayi, V. O. (2012). Modeling the impacts of reforestation on future climate in West Africa. *Theoretical and Applied Climatology*, *110*(1–2), 77–96.

Aguilar, C., Herrero, J., & Polo, M. J. (2010). Topographic effects on solar radiation distribution in mountainous watersheds and their influence on reference evapotranspiration estimates at watershed scale. *Hydrology and Earth System Sciences*, *14*(12), 2479.

Amillo, A. G., Ntsangwane, L., Huld, T., & Trentmann, J. (2018). Comparison of satellite-retrieved high-resolution solar radiation datasets for South Africa. *Journal of Energy in Southern Africa*, *29*(2), 63–76.

Bazyomo, S. D. Y. B., Agnidé Lawin, E., Coulibaly, O., & Ouedraogo, A. (2016). Forecasted Changes in West Africa Photovoltaic Energy Output by 2045. *Climate*, *4*(4), 53.

Bhattacharya, T., Chakraborty, A. K., & Pal, K. (2014). Effects of ambient temperature and wind speed on performance of monocrystalline solar photovoltaic module in Tripura, India. *Journal of Solar Energy*, *2014*.

Burnett, D., Barbour, E., & Harrison, G. P. (2014). The UK solar energy resource and the impact of climate change. *Renewable Energy*, *71*, 333–343. http://doi.org/10.1016/J.RENENE.2014.05.034

Cornforth, R. (2012). Overview of the West African Monsoon 20111. *Weather*, *67*(3), 59–65.

Crook, J. A., Jones, L. A., Forster, P. M., & Crook, R. (2011). Climate change impacts on future photovoltaic and concentrated solar power energy output. *Energy & Environmental Science*, *4*(9), 3101. http://doi.org/10.1039/c1ee01495a

Dee, D. P., Uppala, S. M., Simmons, A. J., Berrisford, P., Poli, P., Kobayashi, S., … others. (2011). The ERA-Interim reanalysis: Configuration and performance of the data assimilation system. *Quarterly Journal of the Royal Meteorological Society*, *137*(656), 553–597.

Déqué, Michel and Calmanti, Sandro and Christensen, Ole Bøssing and Aquila, Alessandro Dell and Maule, Cathrine Fox and Haensler, Andreas and Nikulin, Grigory and Teichmann, C. (2017). A multi-model climate response over tropical Africa at +2 °C. *Climate Services*, *7*, 87–95. http://doi.org/10.1016/J.CLISER.2016.06.002

Diedhiou, A., Bichet, A., Wartenburger, R., Seneviratne, S. I., Rowell, D. P., Sylla, M. B., … others. (2018). Changes in climate extremes over West and Central Africa at 1.5° C and 2° C global warming. *Environmental Research Letters*.

Dubey, S., Sarvaiya, J. N., & Seshadri, B. (2013). Temperature Dependent Photovoltaic (PV) Efficiency and Its Effect on PV Production in the World – A Review. *Energy Procedia*, *33*, 311–321. http://doi.org/10.1016/J.EGYPRO.2013.05.072

ECREEE. (2015). ECOWAs renewable energy Policy. Retrieved September 8, 2018, from http://www.ecreee.org/sites/default/files/documents/ecowas_renewable_energy_policy.pdf

ECREEE. (2016a). Investment Prospectus : General assessment and perspectives Nigeria. Retrieved April 9, 2018, from http://www.ecreee.org/sites/default/files/presentation_of_action_agendas_and_ip_advancements_by_national_directors_for_energy_-_nigeria_-.pdf

ECREEE. (2016b). Investment Prospectus : General assessment and perspectives Sierra Leone. Retrieved April 9, 2018, from http://www.ecreee.org/sites/default/files/presentation_of_action_agendas_and_ip_advancements_by_national_directors_for_energy_-_sierra_leone_-_benjamin_kamara_director_for_energy.pdf

Fesharaki, V. J., Dehghani, M., Fesharaki, J. J., & Tavasoli, H. (2011). The effect of temperature

on photovoltaic cell efficiency. In *Proceedings of the 1stInternational Conference on Emerging Trends in Energy Conservation--ETEC, Tehran, Iran* (pp. 20–21).

Gilani, S. I.-H., Dimas, F. A. R., Shiraz, M., & others. (2011). Hourly solar radiation estimation using ambient temperature and relative humidity data. *International Journal of Environmental Science and Development*, *2*(3), 188–193.

Giorgi, F. (2010). Uncertainties in climate change projections, from the global to the regional scale. *EPJ Web of Conferences*, *9*, 115–129. http://doi.org/10.1051/epjconf/201009009

Gnansounou, E. (2008). Boosting the electricity sector in West Africa: An integrative vision. *International Association for Energy Economics*, *17*, 23–29.

Hagedorn, R., Doblas-Reyes, F. J., & Palmer, T. N. (2005). The rationale behind the success of multi-model ensembles in seasonal forecasting—I. Basic concept. *Tellus A: Dynamic Meteorology and Oceanography*, *57*(3), 219–233.

Houghton, J. T., Ding, Y., Griggs, D. J., Noguer, M., Van Der Linden, P. J., Dai, X., … Johnson, C. A. (2001). Contribution of working group I to the third assessment report of the intergovernmental panel on climate change. *Climate Change 2001: The Scientific Basis*, *388*.

Huber, I., Bugliaro, L., Ponater, M., Garny, H., Emde, C., & Mayer, B. (2016). Do climate models project changes in solar resources? *Solar Energy*, *129*, 65–84. http://doi.org/10.1016/J.SOLENER.2015.12.016

Hulme, M. (2016). 1.5 C and climate research after the Paris Agreement. *Nature Climate Change*, *6*(3), 222.

International Energy Agency (IEA). (2014). Africa Energy Outlook A focus on energy prospects in Sub-Saharan Africa. Retrieved February 4, 2018, from https://www.iea.org/publications/freepublications/publication/WEO2014_AfricaEnergyOutlook.pdf

International Energy Agency (IEA). (2017). Energy Access Outlook 2017 From poverty to prosperity. Retrieved February 3, 2018, from https://www.iea.org/publications/freepublications/publication/WEO2017SpecialReport_EnergyAccessOutlook.pdf

Ishii, T., Otani, K., Takashima, T., & Xue, Y. (2013). Solar spectral influence on the

performance of photovoltaic (PV) modules under fine weather and cloudy weather conditions. *Progress in Photovoltaics: Research and Applications*, *21*(4), 481–489.

Jantsch, M., Stoll, M., Roth, W., Kaiser, R., Schmidt, H., & Schmid, J. (1991). The Effect of Tilt Angle and Voltage Conditions on PV System Performance An Experimental Investigation. In *Tenth EC Photovoltaic Solar Energy Conference* (pp. 431–434).

Jerez, S., López-Romero, J. M., Turco, M., Jiménez-Guerrero, P., Vautard, R., & Montávez, J. P. (2018). Impact of evolving greenhouse gas forcing on the warming signal in regional climate model experiments. *Nature Communications*, *9*(1), 1304.

Jerez, S., Tobin, I., Vautard, R., Montávez, J. P., López-Romero, J. M., Thais, F., … others. (2015). The impact of climate change on photovoltaic power generation in Europe. *Nature Communications*, *6*, 10014.

Kafka, J. L., & Miller, M. A. (2019). A climatology of solar irradiance and its controls across the United States: Implications for solar panel orientation. *Renewable Energy*, *135*, 897–907.

Kazem, H. A., Chaichan, M. T., Al-Shezawi, I. M., Al-Saidi, H. S., Al-Rubkhi, H. S., Al-sinani, K., & Al-Waeli, A. H. A. (2012). Effect of Humidity on the PV Performance in Oman.

Klutse, N. A. B., Ajayi, V. O., Gbobaniyi, E. O., Egbebiyi, T. S., Kouadio, K., Nkrumah, F., … others. (2018). Potential impact of 1.5° C and 2° C global warming on consecutive dry and wet days over West Africa. *Environmental Research Letters*, *13*(5), 55013.

Knippertz, P., Tesche, M., Heinold, B., Kandler, K., Toledano, C., & Esselborn, M. (2011). Dust mobilization and aerosol transport from West Africa to Cape Verde—a meteorological overview of SAMUM-2. *Tellus B*, *63*(4), 430–447.

Kumi, N., & Abiodun, B. J. (2018). Potential impacts of 1.5° C and 2° C global warming on rainfall onset, cessation and length of rainy season in West Africa. *Environmental Research Letters*, *13*(5), 55009.

Mavromatakis, F., Makrides, G., Georghiou, G., Pothrakis, A., Franghiadakis, Y., Drakakis, E., & Koudoumas, E. (2010). Modeling the photovoltaic potential of a site. *Renewable Energy*, *35*(7), 1387–1390.

Mekhilef, S., Saidur, R., & Kamalisarvestani, M. (2012). Effect of dust, humidity and air velocity on efficiency of photovoltaic cells. *Renewable and Sustainable Energy Reviews*, *16*(5), 2920–2925.

Müller, R., Pfeifroth, U., Träger-Chatterjee, C., Trentmann, J., & Cremer, R. (2015). Digging the METEOSAT treasure—3 decades of solar surface radiation. *Remote Sensing*, *7*(6), 8067–8101.

Nikulin, G., Jones, C., Giorgi, F., Asrar, G., Büchner, M., Cerezo-Mota, R., … others. (2012). Precipitation climatology in an ensemble of CORDEX-Africa regional climate simulations. *Journal of Climate*, *25*(18), 6057–6078.

Palmer, T. N. (2016). A personal perspective on modelling the climate system. *Proc. R. Soc. A*, *472*(2188), 20150772.

Panagea, I. S., Tsanis, I. K., Koutroulis, A. G., & Grillakis, M. G. (2014). Climate change impact on photovoltaic energy output: the case of Greece. *Advances in Meteorology*, *2014*.

Parker, D. J., & Diop-Kane, M. (2017). *Meteorology of tropical West Africa: The forecasters' handbook*. John Wiley & Sons.

Patt, A., Pfenninger, S., & Lilliestam, J. (2013). Vulnerability of solar energy infrastructure and output to climate change. *Climatic Change*, *121*(1), 93–102.

Pfeifroth, U., Sanchez-Lorenzo, A., Manara, V., Trentmann, J., & Hollmann, R. (2018). Trends and Variability of Surface Solar Radiation in Europe Based On Surface-and Satellite-Based Data Records. *Journal of Geophysical Research: Atmospheres*, *123*(3), 1735–1754.

Radziemska, E. (2003). The effect of temperature on the power drop in crystalline silicon solar cells. *Renewable Energy*, *28*(1), 1–12.

Riahi, K., Rao, S., Krey, V., Cho, C., Chirkov, V., & Fischer, G. (2011). RCP 8 . 5 — A scenario of comparatively high greenhouse gas emissions, 33–57. http://doi.org/10.1007/s10584-011-0149-y

Riihelä, A., Carlund, T., Trentmann, J., Müller, R., & Lindfors, A. (2015). Validation of CM SAF surface solar radiation datasets over Finland and Sweden. *Remote Sensing*, *7*(6), 6663–6682.

Samouly, A. Al, Luong, C. N., Li, Z., Smith, S., Baetz, B., & Ghaith, M. (2018). Performance of multi-model ensembles for the simulation of temperature variability over Ontario, Canada. *Environmental Earth Sciences*, *77*(13), 524. http://doi.org/10.1007/s12665-018-7701-2

Sawadogo, W., Abiodun, B. J., & Okogbue, E. C. (2019). Projected changes in wind energy

potential over West Africa under the global warming of 1.5° C and above. *Theoretical and Applied Climatology*, 1–13.

Solomon, S., Plattner, G.-K., Knutti, R., & Friedlingstein, P. (2009). Irreversible climate change due to carbon dioxide emissions. *Proceedings of the National Academy of Sciences*, *106*(6), 1704–1709.

Stöckli, R., & Stöckli, R. (2013). *The HelioMont surface solar radiation processing*. Bundesamt für Meteorologie und Klimatologie, MeteoSchweiz.

Sylla, M. B., Elguindi, N., Giorgi, F., & Wisser, D. (2016). Projected robust shift of climate zones over West Africa in response to anthropogenic climate change for the late 21st century. *Climatic Change*, *134*(1), 241–253. http://doi.org/10.1007/s10584-015-1522-z

Sylla, M. B., Gaye, A. T., Jenkins, G. S., Pal, J. S., & Giorgi, F. (2010). Consistency of projected drought over the Sahel with changes in the monsoon circulation and extremes in a regional climate model projections. *Journal of Geophysical Research Atmospheres*, *115*(16), 1–9. http://doi.org/10.1029/2009JD012983

Sylla, M. B., Giorgi, F., Pal, J. S., Gibba, P., Kebe, I., & Nikiema, M. (2015). Projected changes in the annual cycle of high-intensity precipitation events over West Africa for the late twenty-first century. *Journal of Climate*, *28*(16), 6475–6488.

TamizhMani, G., Ji, L., Tang, Y., Petacci, L., & Osterwald, C. (2003). Photovoltaic module thermal/wind performance: long-term monitoring and model development for energy rating. In *NCPV and Solar Program Review Meeting Proceedings, 24-26 March 2003, Denver, Colorado (CD-ROM)*.

Tang, C., Morel, B., Wild, M., Pohl, B., Abiodun, B., & Bessafi, M. (2018). Numerical simulation of surface solar radiation over Southern Africa. Part 1: Evaluation of regional and global climate models. *Climate Dynamics*. http://doi.org/10.1007/s00382-018-4143-1

Touré, N., Konaré, A., & Silué, S. (2012). Intercontinental transport and climatic impact of Saharan and Sahelian dust. *Advances in Meteorology*, *2012*.

UNFCCC. (2015). Paris Agreement: essential elements. Retrieved September 3, 2017, from http://unfccc.int/paris_agreement/items/9485.php

Urraca, R., Gracia-Amillo, A. M., Koubli, E., Huld, T., Trentmann, J., Riihelä, A., … Antonanzas-Torres, F. (2017). Extensive validation of CM SAF surface radiation products

over Europe. *Remote Sensing of Environment*, *199*, 171–186.

van Vuuren, D. P., Edmonds, J., Kainuma, M., Riahi, K., Thomson, A., Hibbard, K., … Rose, S. K. (2011). The representative concentration pathways: an overview. *Climatic Change*, *109*(1), 5. http://doi.org/10.1007/s10584-011-0148-z

Wallach, D., Mearns, L. O., Ruane, A. C., Rötter, R. P., & Asseng, S. (2016). Lessons from climate modeling on the design and use of ensembles for crop modeling. *Climatic Change*, *139*(3–4), 551–564.

Wild, M., Folini, D., Henschel, F., Fischer, N., & Müller, B. (2015). Projections of long-term changes in solar radiation based on CMIP5 climate models and their influence on energy yields of photovoltaic systems. *Solar Energy*, *116*, 12–24. http://doi.org/10.1016/J.SOLENER.2015.03.039

Zang, H., Guo, M., Wei, Z., & Sun, G. (2016). Determination of the optimal tilt angle of solar collectors for different climates of china. *Sustainability*, *8*(7), 654.

Zhou, W., Yang, H., & Fang, Z. (2007). A novel model for photovoltaic array performance prediction. *Applied Energy*, *84*(12), 1187–1198.

Funding information

Funding for this study was provided by the German Ministry for Education and Research (BMBF) through the West African Science Service Center on Climate Change and Adapted Land Use (WASCAL) and by the South African National Research Foundation (NRF).

Conflict of interest

The authors declare that they have no conflict of interest.

- The CORDEX dataset simulates well climate variables needed for calculating PVP over West Africa.
- A decrease in PVP is projected over West Africa due to both global warming and global dimming.
- The magnitude of the decrease grows with global warming levels.
- The arrival of monsoon over each zone weakens the projected decrease in PVP by reducing cloudiness.
- Decreased PVP is projected over most of the selected countries, with a maximum decrease of 3.8% at warming level of 3.0°C.